Project no. GOCE-CT-2003-505539

Project acronym: ENSEMBLES

Project title: ENSEMBLE-based Predictions of Climate Changes and their Impacts

Instrument: Integrated Project

Thematic Priority: Global Change and Ecosystems

Deliverable D4.2.3

Analysis of the land/sea warming ratio in the RT4 coordinated experiments

Due date of deliverable: month 42
Actual submission date: 17 March 2008

Start date of project: 1 September 2004 Duration: 60 Months

Organisation name of lead contractor for this deliverable: UREADMM

Project co-funded by the European Commission within the Sixth Framework Programme (2002-2006)		
Dissemination Level		
PU	Public	PU
PP	Restricted to other programme participants (including the Commission Services)	
RE	Restricted to a group specified by the consortium (including the Commission Services)	
CO	Confidential, only for members of the Consortium (including the Commission Services)	

1. Introduction

Coupled atmosphere ocean general circulation models (CGCM) are among the most powerful tools to both enhance our understanding of the fundamental mechanisms of the climate system and make projections of future climate change. The responses of surface air temperature and precipitation of these models to increasing greenhouse gases (GHG) have been studied extensively and summarized in the Third and Fourth Assessment Report of the Intergovernmental Panel on Climate Change (IPCC TAR, Houghton et al. 2001, IPCC AR4 Solomon et al. 2007). Most CGCMs show some similar features of the surface air temperature changes. For example, the greatest warming occurs over the high latitudes of the winter hemisphere. Feedbacks associated with sea ice and snow cover are widely accepted as being the main cause of this polar amplification (e.g., Hansen et al. 1997, Hall 2004) although recent studies suggest that other processes are also important (Alexeev et al., 2005; Winton, 2006).

Using IPCC AR4 model integrations, Sutton et al. (2007) investigated the tendency for greater warming over land than over sea in response to greenhouse gas forcing. In all the 20 CGCMs examined warming over land exceeds warming over sea, i.e. the land/sea warming ratio is greater than 1 (the land/sea warming ratio is the global mean surface air temperature change over land regions divided by the global mean surface air temperature change over ocean regions. For brevity this quantity is henceforth referred to as simply "the warming ratio"). They have further illustrated that, for any given model, the warming ratio in the presence of increasing radiative forcing is fairly constant in time, implying that the land/sea temperature difference increases with time. Furthermore, the enhanced warming over land is not principally a transient effect caused by the greater heat capacity of the ocean; although this is a contributory factor, the contrast is present to nearly the same extent if CO_2 is held constant at twice its initial value in CGCM integrations, and in equilibrium conditions for double CO_2 in models with mixed-layer ("slab") oceans. They also showed that global mean warming ratios for the CGCMs are in the range 1.36 – 1.84. This level of uncertainty is comparable to that in global mean temperatures (i.e. climate sensitivity) and has significant implications for climate impacts. Analysis to date points to the potential importance of land surface and cloud feedbacks but the reasons different models give different ratios are not fully understood. One of the uncertainties of simulated land sea warming ratio is associated with the amplitude and the pattern of SST change induced by climate change forcing. It is, therefore, expected that the uncertainty of land sea warming ratios shall be reduced in atmospheric models if they are

forced by same SST changes. The research theme 4 (RT4) coordinated experiments repeated with several different atmospheric GCMs within the ENSEMBLES project will help us to advance understanding of the factors and processes controlling future climate changes and related uncertainty in climate forecasts.

In this report we use these experiments to try to understand the mechanisms responsible for the land sea warming contrast and its uncertainty. The key questions we aim to address are: 1) What are the global land-sea warming ratios and what determines these ratios in response to an increase of greenhouse gases concentration? 2) Does the range of land sea warming ratio of atmospheric GCMs reduce, relative to coupled models, when they are forced by the same SST and CO_2 changes? 3) What are the characteristics of latitudinal variations of the land/sea warming ratio and its seasonal evolution? 4) What is the role of land surface feedback?

In section 2, the models and experiments are described. The comparison of changes in surface air temperature and global land sea warming contrast among models is described in section 3. The change of land sea warming contrast with height is illustrated in section 4 and its latitudinal variation is investigated in section 5. The seasonal cycle of land sea warming ratio at the surface is studied and compared with observations in section 6 and conclusions are in section 7.

2. Models and experiments

2.1 ENSEMBLES RT4 coordinated time-slice experiments

Broad aims:

a. Understanding climate, and climate forecast uncertainty at a mechanistic/process level, particularly in terms of the role of specific feedbacks, the regional patterns of climate change, and the factors governing the frequency and characteristics of extreme events.

b. Add value to information available from core ENSEMBLES hindcasts, forecasts and scenario integrations.

c. Need a simple core set of computationally cheap experiments so that they can be done by all groups (including where possible different model resolutions etc).

Proposed scientific focus

With respect to climate forecast uncertainty, coordinated experiments focus on understanding model uncertainty (rather than scenario uncertainty or initial condition uncertainty) since that is where such experiments can most obviously add value. A major but not exclusive scientific focus should be understanding the factors that determine the land sea-warming contrast and understanding the spread of the warming ratio seen in IPCC AR4 models (Sutton et al. 2007). By using the atmospheric GCMs forced by same SST and CO_2 changes, we can focus on understanding the uncertainty associated with atmospheric and land surface feedbacks.

Experiments

Control and a $2xCO_2$ experiments were conducted using common time invariant, SST and ice fields as lower boundary conditions; these boundary conditions were derived from a coupled experiment with the Hadley Centre model. The purpose of using common lower boundary conditions is to remove some sources of inter-model variance (e.g. sea ice-albedo feedback) in order to better understand others. For control experiments, climatological monthly mean SST and sea-ice concentrations derived from HadISST observations for 1961-1990 and CO_2 at average concentration for 1961-1990. For perturbed experiments ($2xCO_2$), monthly mean SST anomalies are added to climatological fields used for control experiments. SST anomalies are derived from 1% pa CO_2 CMIP-type integration with HadCM3 model. The difference between two 30 year means: a) mean for period with CO_2 values near present day and b) mean for period with values near 2 x present day CO_2 are used. For perturbation experiments, sea ice extent is taken from HadCM3 model of 30 year mean for the period with values near 2 x present day CO_2. For each of control and perturbed experiments, 2 x 25 year integrations with different initial conditions have been performed. The first 5 year of each integration has been ignored and this gives 40 years of data to analyse for each experiment.

2.2 Groups participating in ENSEMBLES RT4 coordinated experiments

The groups participating in ENSEMBLES RT4 coordinated experiments and the main features of models used are given in Table 1. There are 8 participating groups and the simulations of 7 models from 6 groups are archived in the database. Abdus Salam ICTP has performed simulations and they are archived in the database, but the coarse resolution of this model is not appropriate for analysing and understanding land sea warming contrast and therefore results from this model are not included in present study. UREADMM has performed an additional $2xCO_2$ experiment using HadAM3 without the change in stomatal

resistance. This additional simulation is used in this analysis, but not archived in database. However, it can be made available for researchers upon request from the partner UREADMM.

Table 1: The main features of models used and the references. Models with a change in stomatal resistance in response to double CO_2 are with a phrase "with variable SR" while models without a change in stomatal resistance are with a phrase "with fixed SR".

Partners	Group	Model	Reference	Model experiment abbreviation
CNRM	Centre National de Recherches Meteorologiques, France	CNRM-CM3, T42 with fixed SR	Salas-Melia et al. (2005)	cnrm_cm3
CERFACS	Centre Europeen de Recherche et de Formation Avancee en Calcul Scientifique, France	ARPEGE-climate v4 T63 with fixed SR	Deque (2003)	cerfacs_arpv4
INGV	Istituto Nazionale di Geofisicae Vulcanologia Italy	ECHAM4 T42 ECHAM4 T106 with fixed SR	Roeckner (1996)	ingv_t42 ingv_t106
UREADMM	NCAS-Climate, University of Reading, UK	HadAM3 (2.5x3.75) with variable SR HadAM3 with fixed SR	Pope et al.(2000)	cgam_hadam3 cgam_hadam3s
IPSL	Centre National de la Recherche Scientifique France	IPSL-CM4 (2.5x3.75) with variable SR	Marti et al.(2005)	ipsl_cm4
ICTP	Abdus Salam ICTP, Italy	ICTP-AGCM T30/L8	Molteni (2003)	ictp_speedy
ifM-Kiel	Institut fur Meereskunde, Germany	ECHAM5 T106		not done yet
NERSC	Nansen Environmental and Remote Sensing Center, Norway	ARPEGE V3.1 T63/L31		not done yet

3. Global land sea warming contrast

a. Surface air temperature change

Figure 1 shows the multi-model ensemble mean annual surface air temperature change in response to imposed SST change and doubling CO_2. The multimodel mean shows the familiar pattern of enhanced warming over land and over high northern latitudes, the latter being partly associated with regions of reduced sea-ice and snow cover. Over land the warming has similar magnitude (2-3^oC) over Africa, Australia, and South America. The largest warming of 4-5^oC occurs over North America and high latitude of Eurasian continent. These features are similar

to the results based on IPCC AR4 model (Sutton et al. 2007). The cooling around sea ice edge in high latitudes of the southern hemisphere from 90°E to 160°W and over small region over Artic is a result of prescribing sea ice edge for $2xCO_2$ experiment based on HadCM3 simulation while it is based on observations for the control experiment. Because of this, the sea ice edge is further equatorward in some longitudes in $2xCO_2$ experiment relative to the control experiment. We have performed a sensitivity experiment using HadAM3 to test the role of this equatorward displacement of sea ice edge in these longitudes on global climate. It has been shown that its global impact and remote regional impact is small and not significant despite its significant local effect.

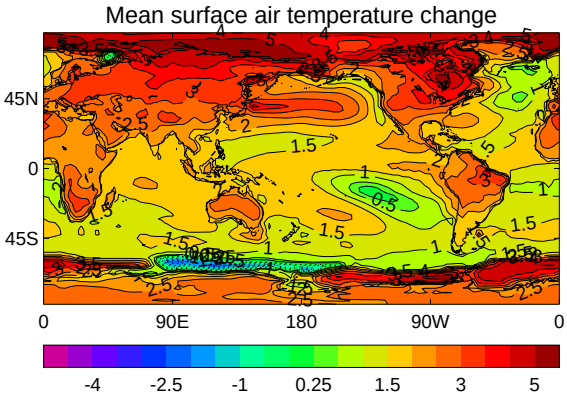

Figure 1: The multi-model ensemble mean annual surface air temperature change (Unit: °C) between $2xCO_2$ and control experiments. (7 model simulations participated in ENSEMBLES RT4 coordinated experiments are listed in Table 1)

Figure 2 shows the global mean temperature change over land and over ocean and the land sea warming ratio for individual models. The temperature change over land ranges from 2.47 to 3.19 with a mean of 2.75 and standard deviation of 0.23. The warming ratio ranges from 1.54 (CERFACS-ARPV4) to 1.78 (HadAM3) with a mean of 1.61 and standard deviation of 0.08. This range of the warming ratio is smaller than that obtained from IPCC AR4 models that show a warming ratio range from 1.36 to 1.84 with a mean of 1.55 and standard deviation of 0.13 (Sutton et al. 2007). The mean difference between multimodel mean warming ratio obtained using the ENSEMBLES RT4 coordinated experiments and that obtained from the IPCC AR4 models are not statistically significant. However, the difference of warming ratio standard deviation among two groups of models is statistically significant at 99% confidence level using F-test. These results indicate that uncertainty of land sea warming ratio is reduced in the atmospheric models forced by same SST change and imply that one factor responsible for large spread of land sea warming ratio in response to greenhouse gas changes in IPCC AR4 model is uncertainty of the magnitude and spatial pattern of SST change in response to forcing in these coupled models.

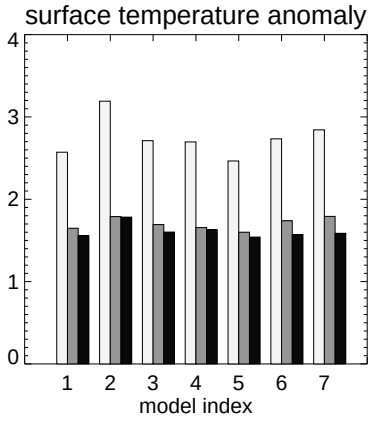

Figure 2: Annual mean surface air temperature changes over land (white bar), over sea (grey bar), and the land sea warming ratios (black bar) between $2xCO_2$ and control simulations in the ENSEMBLES RT4 coordinated experiments. 1 for cnrm_cm3, 2 for cgam_hadam3, 3 ingv_t42, 4 for ingv_t106, 5 for cerfacs_arpv4, 6 for ipsl_cm4, and 7 for cgam_hadam3s.

The direct response to the CO_2 change has two components, one associated with purely radiative effects and the other associated with the reduction in stomatal resistance. The reduction in stomatal resistance inhibits transpiration, and thus surface evaporative cooling. By comparing two HadAM3 simulations (one with the change in stomatal resistance and the other without the change in it), we can assess the relative role of the change of stomatal resistance on land surface warming.

Figure 3 shows the global annual mean temperature change resulting from the change in stomatal resistance. It clearly indicates that the reduction in stomatal resistance leads to warming about 0.25-0.75^{o}C in large areas over global continents with a global mean warming 0.35^{o}C. The largest warming of about 0.75-1.0^{o}C occurs over mid-latitude of Asian continent, North America, and South America. Seasonal evolution of the warming pattern indicates that warming associated with the change in stomatal resistance has a strong seasonal cycle with largest warming occurring over continents in summer hemisphere.

As indicated in Figure 2, with fixed stomatal resistance, the global land surface warming in HadAM3 is more in line with those models that do not include the impact of the change in stomatal resistance. This clearly indicates a role of change in stomatal resistance on land surface warming in response to CO_2 change and may imply that the change in stomatal resistance in land surface schemes among different models in response to CO_2 change is another factor that might be responsible for the uncertainty of land sea warming ratio seen in IPCC AR4 models.

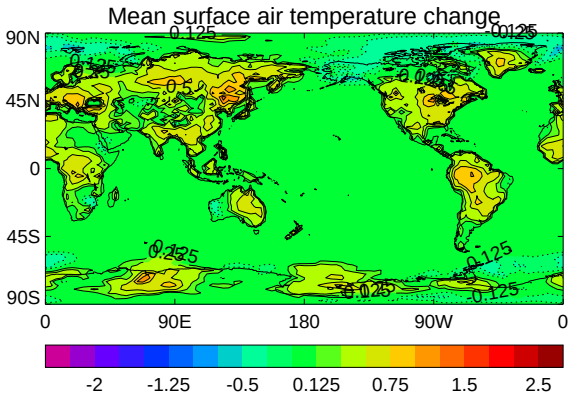

Figure 3: Annual mean surface air temperature change due to the change in stomatal resistance in response to double CO_2 by using HadAM3 model.

b. Change in global surface energy balance

Figure 4 shows the changes in the surface energy budget, over land and over oceans, for all model simulations in response to imposed SST and CO_2 changes. Note that over land the anomalous heat budget sums close to zero (figure 4e) except two simulations with INGV-T42 and INGV-T106, but over the ocean there is a residual reflecting the fact that the experiments are not in equilibrium.

The changes in global surface energy budget show that SST change and doubling CO_2 lead to longwave warming with a multimodel mean of 1.2 W m^{-2} over land and 3.7 W m^{-2} over ocean. All models show longwave warming over ocean and over land. The only exception is the HadAM3 simulation shows weak longwave cooling over land. An increase in downward longwave radiation (as is seen over the ocean surface) is an expected consequence of an enhanced Greenhouse Effect (caused by the elevated CO_2 but importantly amplified by water vapour feedback). The fact that *net* longwave anomalies are small over the land surface suggests that increased emission (in response to the surface warming) offsets increased absorption. The change in longwave in the HadAM3 simulation with the change in stomatal resistance, which also shows the largest land surface warming, indicates that increased longwave emission completely offsets increased absorption.

Figure 4 also shows an enhanced latent heat loss and a decrease in the sensible heat loss for all models over ocean, with a multimodel mean change of -2.8Wm^{-2} and 1.4Wm^{-2}, respectively. Over the land the latent heat loss increases in 5 models and decreases in 2 models (HadAM3 and IPSL-CM4). The decrease in evaporation in these two models is the result of the reduction in stomatal resistance in response to double CO_2 while this impact is not included in

other 5 model experiments. Upward sensible heat flux increases in 5 models with the largest increase in HadAM3 while it decreases in 2 models (INGV-T42 and INGV-T106) it is not clear why upward sensible heat flux decreases when land surface warms in these two models. There is also a large variation of surface shortwave radiation among models over land and ocean with HadAM3 showing the largest increase over land. Lastly, it is notable that turning off the change in stomatal resistance in HadAM3 changes the sign of the latent heat flux, and also has significant effects on the other components of the surface energy budget.

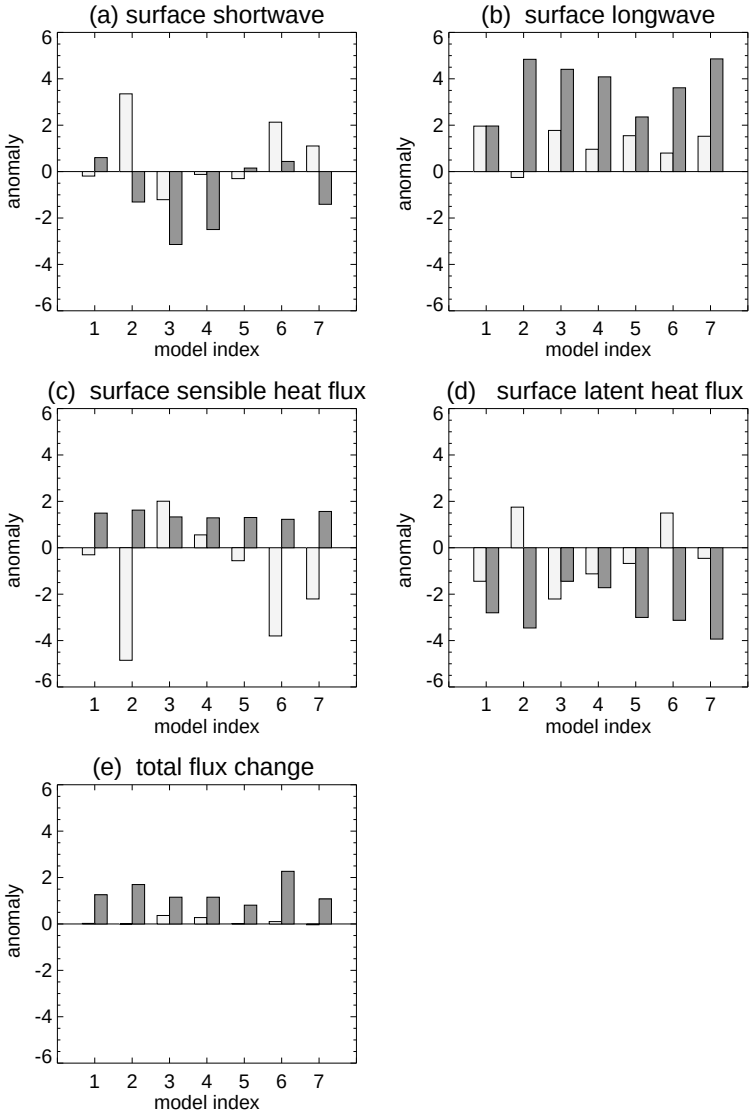

Figure 4: The global mean surface energy anomalies (W m^{-2}) over land (white bar) and sea (grey bar) between the $2xCO_2$ and control simulations in the ENSEMBLES RT4 coordinated experiments. 1 for cnrm_cm3, 2 for cgam_hadam3, 3 ingv_t42, 4 for ingv_t106, 5 for cerfacs_arpv4, 6 for ipsl_cm4, and 7 for cgam_hadam3s. Sign convention is that positive values imply warming the surface.

c. Changes in the hydrological cycle

Closely related to changes in the surface energy balance are changes in the hydrological cycle. Important aspects of these changes are summarized for all models in Figure 5. The most obvious change is the increase in total precipitable water in all models over both land and ocean, as expected for a warmer atmosphere (Held and Soden 2006)**.** As is also expected, warm SSTs and double CO_2 lead to an increase in precipitation (Fig. 5b) over ocean. However, precipitation change over land shows a large spread with model IPSL-CM4 showing very weak increase and CNRM-CM4 and INGV-T42 showing similar increase to that over ocean. One important feature is that anomalous precipitation and evaporation is local with respect to land and sea for most models as indicated by very small anomalies of precipitation minus evaporation (P-E) over land and sea (Fig. 5d) except models HadAM3 and IPSL-CM4. In these two models, large P-E anomalies over both land and ocean imply there are enhanced moisture transport from ocean to land in response to the imposed changes in SST and CO_2.

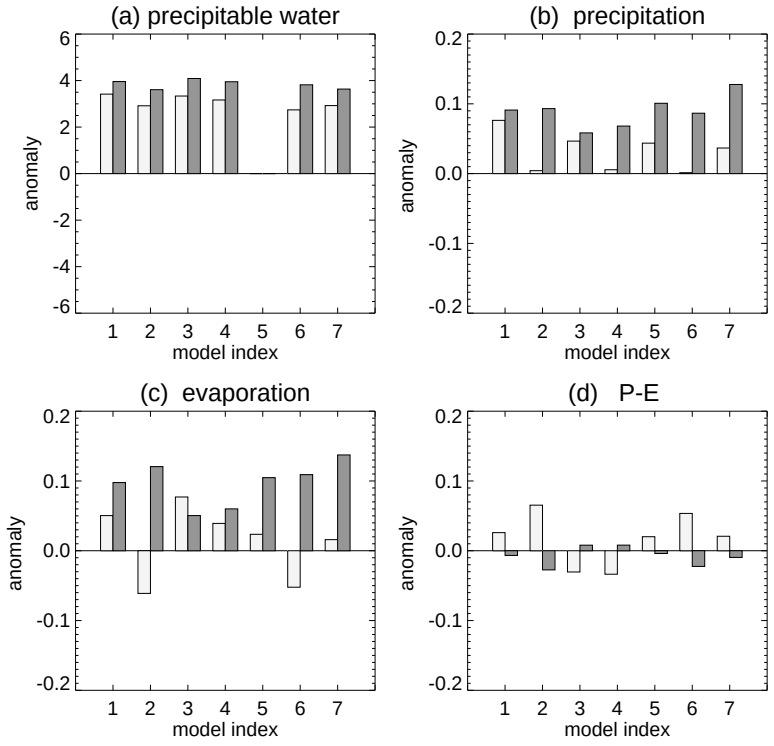

Figure 5: The global mean anomalies of hydrological variables over land (white bar) and sea (grey bar) between the 2xCO_2 and control simulations in the ENSEMBLES RT4 coordinated experiments. 1 for cnrm_cm3, 2 for cgam_hadam3, 3 ingv_t42, 4 for ingv_t106, 5 for cerfacs_arpv4, 6 for ipsl_cm4, and 7 for cgam_hadam3s. Units are kg m^{-2} in (a) and mm day^{-1} in (b), (c) and (d).

4. Vertical structure of temperature changes and land sea warming ratio

Shown in figure 6 are the vertical profiles of temperature anomalies averaged over land and ocean. As figure 6b indicates, all models show a warming of troposphere temperature with relative maximum at the upper troposphere over ocean in response to imposed SST and CO_2 changes. The strongest warming of about 3^oC in the upper troposphere at about 300 hPa is associated with the largest fractional increase (40%-60%) of upper tropospheric water vapour (not shown) which is in contrast with about 10%-15% increase near the surface and in lower troposphere. This is because warm SSTs enhance energy and moisture fluxes into the atmosphere, which destabilise the atmospheric boundary layer over ocean, and builds up convective available potential energy (CAPE) for organising deep convection. The enhanced deep convection leads to large warming and moistening of the upper troposphere over ocean. As figure 6b shows, the spread of temperature change among models is weak in the lower troposphere because of the constraint of the same SST change. However, the spread of temperature change in upper troposphere is relatively large, presumably related to differences in the representation of water vapour, lapse rate and other feedbacks.

The vertical profiles of temperature changes over global land show some distinct features from the ocean. All models indicate a surface amplification of the land warming with relative large spread among models, implying a role of local feedbacks. As over ocean, figure 4a shows another warming maximum in the upper troposphere over land. This is due to the fact that the large-scale dynamics acts to spread the heating over ocean across the entire tropical belt (Sobel et al. 2002, Chiang and Lintner 2005) because the tropical atmosphere cannot maintain strong temperature gradient. These results are consistent with the conceptual model proposed by Joshi et al. (2008).

As figure 6c shows, the enhanced warming over land not only happens at the surface, but also extends into free troposphere. All models show that the land sea warming ratios are the largest at the surface and decrease rapidly with height in the lower troposphere with land sea warming contrast being very small above 750 hPa.

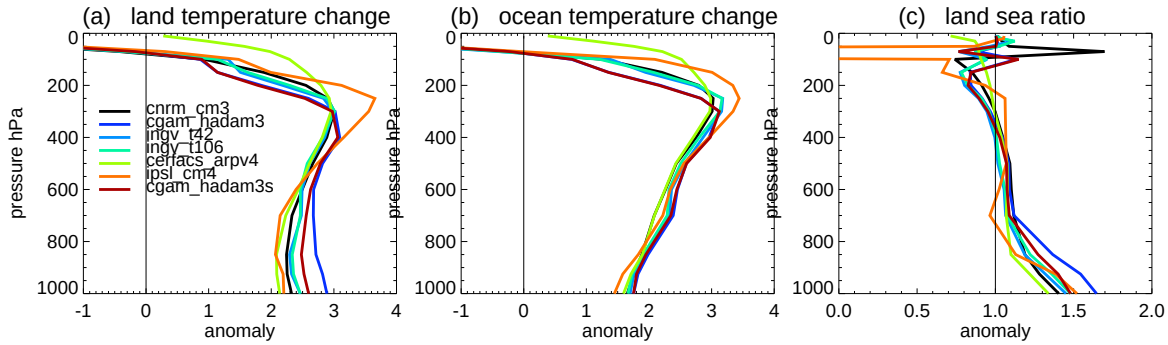

Figure 6: The vertical distribution of global mean temperature change (°C) between the 2xCO2 and control simulations in the ENSEMBLES RT4 coordinated experiments. (a) over land, (b) over ocean, and (c) land sea warming ratio.

5. Latitudinal dependence of temperature change and warming ratio

Figure 7 shows how the surface warming over land, over ocean and the land sea warming ratio vary with latitude in all model simulations. Large warming occurs over high latitudes in both hemispheres over ocean and land. This polar amplification is generally attributed to snow and sea ice albedo feedback, although recent studies suggest that other processes are also important (e.g., Hansen et al., 1997; Hall, 2004; Holland and Bitz, 2003; Alexeev et al., 2005; Winton, 2006).

The land sea warming ratios, as illustrated in figure 7c, indicate a very consistent pattern in the lower latitudes, with a minimum (multimodel mean ratio ~1.2) in equatorial latitudes, and maxima (~1.5-2.2) around 15°S. This consistent pattern of latitudinal variation of warming ratio among models is expected from the simple theory highlighted by Sutton et al. (2007). The theory indicates the warming ratio to be higher in regions where land is relatively dry, and lower in regions where land is relatively wet.

The role of the change in stomatal resistance is also illustrated in figure 7 by the two HadAM3 simulations. With the change in stomatal resistance, the land sea warming ratios in HadAM3 are the largest in the tropics and subtropics, while with fixed stomatal resistance, the ratios are more in line with other models. This clearly indicating the role of the change in stomatal resistance on the spread of latitudinal variation of land sea warming contrast.

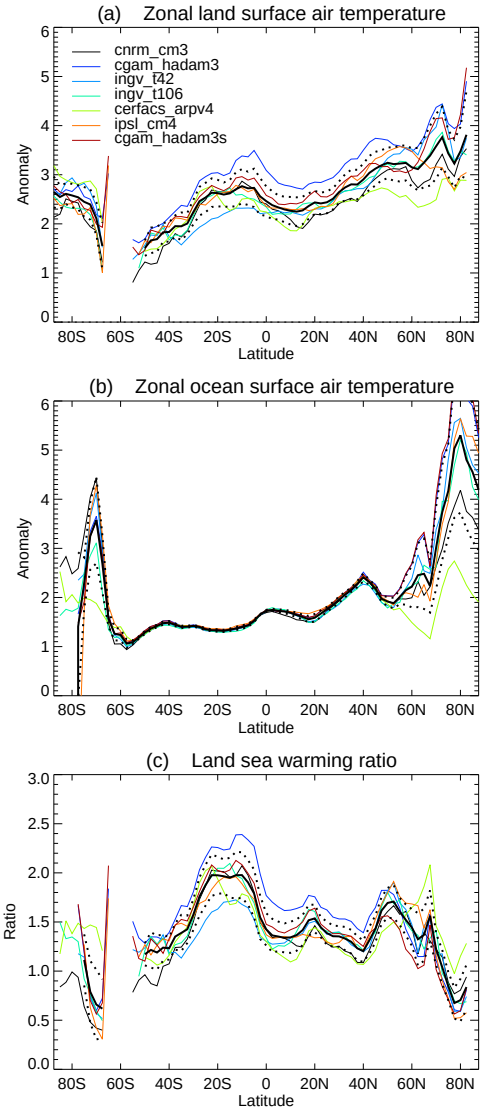

Figure 7: Latitudinal distribution of surface air temperature anomalies (^{o}C) between the 2xCO2 and control simulations in the ENSEMBLES RT4 coordinated experiments. (a) over land, (b) over ocean, and (c) land sea warming ratio. The thick full line is the multimodel mean, and thick dotted lines show one standard deviation variation.

6. Seasonal cycle of warming over land and land sea warming ratio

The seasonal cycles of surface air temperature changes in response to the imposed SST and CO_2 changes over land and ocean are illustrated in figure 8. In general, seasonal cycle of surface air temperature change over ocean is weak (figure 8b). In contrast, there are weak seasonal cycles of surface air temperature changes over land as shown in figure 8a. As a result, the seasonal cycle of land sea warming ratio for each individual model follows closely on the seasonal cycle of land surface warming. Two (HadAM3 with variable stomatal

resistance and IPSL-CM4) of 7 model simulations show there is a weak seasonal cycle of land sea warming ratio with the largest warming ratio occurring in the boreal summer (figure 8c) while other 5 models show the largest warming ratio occurring in the later boreal winter. The enhanced land surface warming in the boreal summer in these two model simulations are associated with the reduction of evaporative cooling with the largest reduction occurring in boreal summer (not shown) related to the change in the stomatal resistance while other 5 models show enhanced evaporative cooling all year round with a weak seasonal cycle. This implies the important role of change of stomatal resistance on the simulated seasonal cycle of land sea warming ratio.

During the last 20-25 years, sea surface temperature and land air temperature have a warming trend with the warming over land being grater than over ocean (Kumar et al. 2004, Sutton et al. 2007). Figure 8a and b also show the seasonal cycles of linear trends of global surface air temperature over land and sea surface temperature over ocean based on observations (HadCRUT3v, Jones et al., 2001) for the period 1980-2004. As figure 8a indicates, the warming trend over land has a maximum in boreal winter. The enhanced warming trend in boreal winter may indicate a significant component of natural variability. As discussed in Folland et al (2001), recent warming (1976 to 2004) has been greatest over the mid-latitude Northern Hemisphere continents in winter, and a component of the signal may be explained by the sharp increase in the positive phase of the North Atlantic Oscillation (NAO) / Northern Annular Mode (NAM) (e.g., Hurrell, 1995; Thompson et al., 2000) since about 1970 (though the change in the NAO/NAM may itself have had an anthropogenic component). The linear warming trend over ocean shows a weak seasonal cycle. As a result, the ratio of the linear warming trend over land to that over ocean (figure 8c) based on observations in boreal winter is larger than other seasons. However, this land sea warming ratio based on observations in other seasons are very close to the warming ratio from the models, possibly implying that land/sea warming contrast is a signal of anthropogenic warming (Braganza et al. 2004).

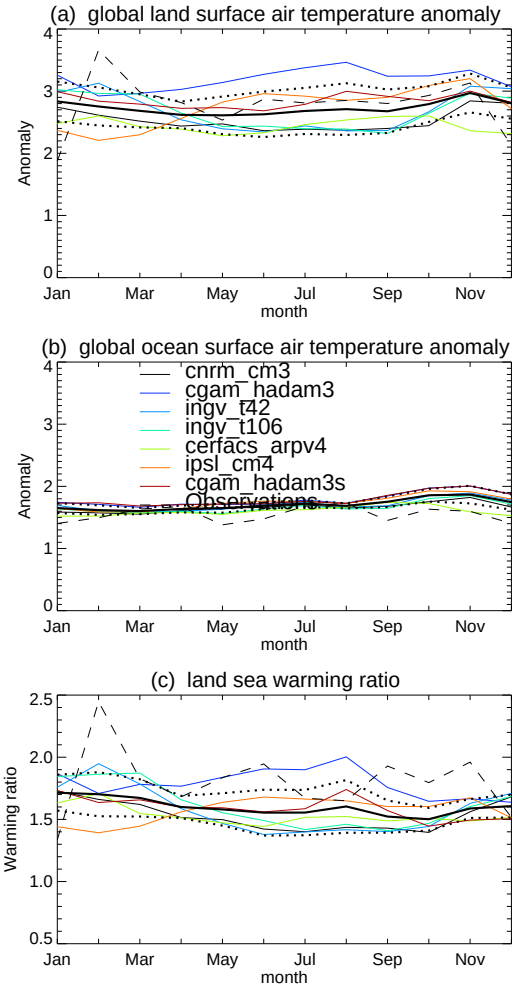

Figure 8: The seasonal cycle of global mean surface air temperature change (^{o}C) between the 2xCO2 and control simulations in the ENSEMBLES RT4 coordinated experiments. (a) over land, (b) over ocean, and (c) land sea warming ratio. The thick full line is the multimodel mean, and thick dotted lines show one standard deviation variation. Shown in observations are linear trends (^{o}C century^{-1}) based on HadCRUT3v data for the period 1980-2004, calculated from combined land-surface air and sea surface temperatures adapted from Jones et al. (2001).

To exclude to uncertainty associated with high latitude snow sea ice feedback among models, figure 9 shows the seasonal cycle of surface air temperature changes over land, over ocean and the land sea warming ratio in the tropics and subtropics. As figure 9a indicates, seasonal evolution of land surface temperature changes in the tropics and subtropics are more consistent among models, and show enhanced warming in boreal spring and summer and weaker warming in boreal winter. The seasonal cycle of land sea warming ratio in individual model follows the seasonal cycle of land surface warming and shows weak seasonal cycle with large land sea warming ratio occurring in boreal summer.

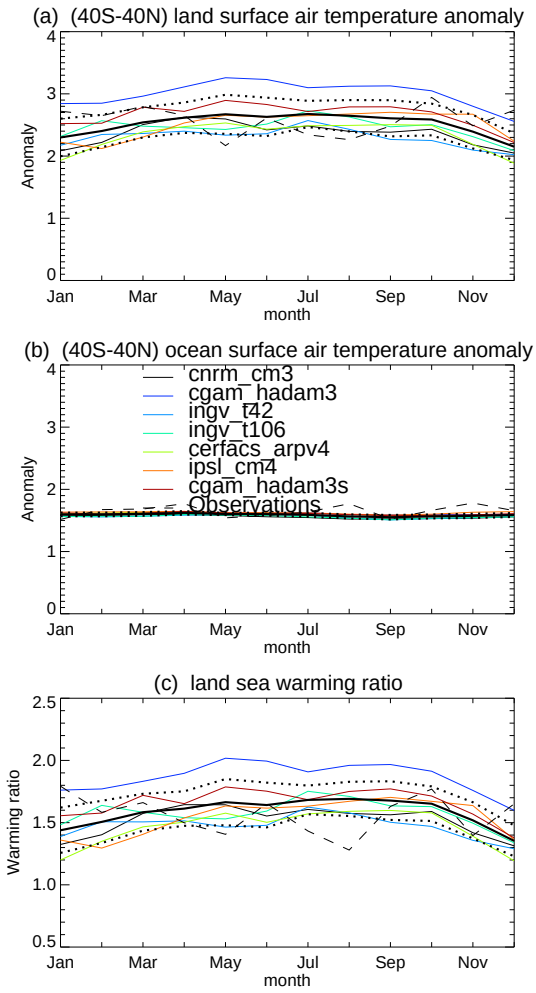

Figure 9: The seasonal cycle of mean surface air temperature change (^{o}C) in the tropics and subtropics between the 2xCO2 and control simulations in the ENSEMBLES RT4 coordinated experiments. (a) over land, (b) over ocean, and (c) land sea warming ratio. The thick full line is the multimodel mean, and thick dotted lines show one standard deviation variation. Shown in observations are linear trends (^{o}C century^{-1}) based on HadCRUT3v data for the period 1980-2004, calculated from combined land-surface air and sea surface temperatures adapted from Jones et al. (2001).

7. Conclusions

Using ENSEMBLES RT4 coordinated experiments we have investigated the tendency for greater warming over land than over sea in response to greenhouse gas forcing. In all the 7 models examined warming over land exceeds warming over sea, i.e. the land/sea warming ratio is greater than 1. The warming ratio ranges from 1.54 to 1.78 with a mean of 1.61 and standard deviation of 0.08 in the ENSEMBLES RT4 experiment. This range of the warming ratio is smaller than those obtained from IPCC AR4 models that show a warming ratio range from 1.36

to 1.84 with a mean of 1.55 and standard deviation of 0.13 (Sutton et al. 2007). The small spread of the warming ratio in the ENSEMBLES RT4 experiments indicate that uncertainty of land sea warming ratio is reduced in the atmospheric models forced by same SST change. This implies that one factor responsible for large spread of land sea warming ratio in response to greenhouse gas changes in IPCC AR4 model is the uncertainty of magnitude and spatial pattern of SST change in the coupled models.

All models show that the largest land-sea warming occurs at the surface. The ratio decreases with height and approaches 1 at middle troposphere and becomes less than 1 in the upper troposphere. This robust feature among different models suggests a simple mechanism operating in all models and is consistent with the concept model proposed by Joshi et al. (2007).

The land/sea warming ratio varies with latitude, showing a minimum in equatorial latitudes, and maxima in the subtropics. This latitude variation of the warming ratio is more consistent in the current experiments than that shown in figure 4 of Sutton et al. (2007) based on IPCC AR4 results. This implies a role for the SST pattern in individual models in determining the latitudinal distribution of land sea warming ratio seen in IPCC AR4 models. This consistent pattern of latitudinal variation of warming ratio among models is expected from the simple theory highlighted by Sutton et al. (2007). The theory indicates the warming ratio to be higher in regions where land is relatively dry, and lower in regions where land is relatively wet.

Two (HadAM3 with variable stomatal resistance and IPSL-CM4) of 7 model simulations show there is a weak seasonal cycle of land sea warming ratio with the largest warming ratio occurring in the boreal summer while other 5 models show the largest warming ratio occurring in the later boreal winter. The enhanced land surface warming in the boreal summer in these two model simulations are associated with a reduction of evaporative cooling, which is the largest in boreal summer, while the other 5 models show enhanced evaporative cooling all year round with a weak seasonal cycle. This implies the important role of change of stomatal resistance on the simulated seasonal cycle of land sea warming ratio. Detailed analysis to understand the reasons for the differences among all models will be ongoing.

The fact that warming over land is more rapid than over sea is clearly important for climate impacts, since people live on land. Our study suggests that further work is needed to understand the causes of the land/sea contrast in surface warming, the variation of this quantity between models, and the consequences of the associated uncertainty for climate impacts. The

specific prediction that the land/sea temperature difference should increase as the planet warms could imply specific impacts which merit investigation, e.g. effects on the large scale circulation [e.g., Jain et al., 1999] or local effects such as stronger sea breezes. There is also a potential for important interactions with changes in the hydrological cycle, such as the apparent land/sea contrast in precipitation trends [Bosilovich et al., 2005].

Acknowledgment *Financial support by the EU FP6 Integrated Project ENSEMBLES (Contract number 505539) is gratefully acknowledged.*

References

Alexeev, V. A., P. L. Langen and J. R. Bates, 2005: Polar amplification of surface warming on an aquaplanet in "ghost forcing" experiments without sea ice feedbacks. *Clim. Dyn.*, 24, 655-666. DOI: 10.1007/s00382-005-0018-3.

Bosilovitch, M.G., S.D. Schubert and G.K. Walker, 2005: Global Changes of the Water Cycle Intensity, *J. Climate*, 18, 1591-1608.

Braganza, K., D.J. Karoly, A.C. Hirst, P. Stott, R.J. Stouffer and S.F.B. Tett, 2004: Simple indices of global climate variability and change Part II: attribution of climate change during the twentieth century, *Clim. Dyn*., 22, 823-838. DOI: 10.007/s00382-004-0413-1.

Chiang, J. C. H. and B. R. Lintner, 2005: Mechanisms of remote tropical surface warming during El Nino. *J. Climate*, 18, 4130-4149.

Cubasch, U., and Coauthors, 2001: Projections of future climate change. *Climate Change 2001: The Scientific Basis. Contribution of Working Group I to the Third Assessment Report of the Intergovernmental Panel on Climate Change,* J. T. Houghton, et al., Eds., Cambridge University Press, 525–582.

Deque, M., 2003: ARPEGE-Climate Version 4. Algorithmic Documentation. 365 pp.

http://www.cnrm.meteo.fr/gmapdoc/modeles/docus.html.

Folland, C., T. R. Karl and Coauthors, 2001: Observed Climate Variability and Change. *Climate Change 2001: The Scientific Basis. Contribution of Working Group I to the Third Assessment Report of the Intergovernmental Panel on Climate Change,* J. T. Houghton, et al., Eds., Cambridge University Press, 101–181.

Hall, A ., 2004: The role of surface albedo feedback in climate. *J. Climate*, 17, 1550-1568.

Hansen, J., M. Sato and R. Ruedy, 1997: Radiative forcing and climate response. *J. Geophys. Res*., 102(D6), 6831–6864.

Held, I. M., and B. J. Soden, 2006: Robust responses of the hydrological cycle to global warming. *J. Climate*, 19, 5686-5699.

Hurrell, J.W., 1995: Decadal trends in the North Atlantic Oscillation regional temperatures and precipitation. *Science*, 269, 676-679.

IPCC, 2001: Climate Change 2001: The Scientific Basis. *Contribution of Working Group I to the Third Assessment Report of the Intergovernmental Panel on Climate Change*. Houghton, J.T. et al., Eds. Cambridge University Press, 881 pp.

IPCC, 2007: Climate Change 2007: The Scientific Basis. *Contribution of Working Group I to the Fourth Assessment Report of the Intergovernmental Panel on Climate Change* Solomon, S.D. et al., Eds. Cambridge University Press, 996 pp.

Jones, P.D., T.J. Osborn, K.R. Briffa, C.K. Folland, E.B. Horton, L.V. Alexander, D.E. Parker and N.A. Rayner, 2001: Adjusting for sampling density in grid box land and ocean surface temperature time series. *J. Geophys. Res*., **106**, 3371-3380.

Joshi, M., J. Gregory, M. Webb, D. Sexton, and T. Johns, 2008: Mechanisms for the land/sea warming contrast exhibited by simulations of climate change. *Clim. Dyn*., 30, 455-465. doi:10.1007/s00382-007-0306-1.

Kumar, A., F. Yang, L. Goddard, and S. Schubert, 2004: Differing trends in the tropical surface temperatures and precipitation over land and oceans, J. Clim., 17, 653-664.

Lintner, B. R., and J. C. H. Chiang, 2007: Adjustment of the remote tropical climate to El Nino conditions. *J. Climate*, 20, 2544-2557.

Marti, O and others, (2005): The new IPSL climate system model: IPSL-CM4. http://dods.ipsl.jussieu.fr/omamce/IPSLCM4/DocIPSLCM4/FILES/DocIPSLCM4.pdf.

Meehl, G.A., T.F. Stocker, W.D. Collins, P. Friedlingstein, A.T. Gaye, J.M. Gregory, A. Kitoh, R. Knutti, J.M. Murphy, A. Noda, S.C.B. Raper,I.G. Watterson, A.J. Weaver and Z.-C. Zhao, 2007: Global Climate Projections. In: *Climate Change 2007: The Physical Science Basis. Contribution of Working Group I to the Fourth Assessment Report of the Intergovernmental Panel on Climate Change* [Solomon, S.,D. Qin, M. Manning, Z. Chen,

M. Marquis, K.B. Averyt, M. Tignor and H.L. Miller (eds.)]. Cambridge University Press, Cambridge, United Kingdom and New York, NY, USA.

Molteni, F., 2003:Atmospheric simulations using a GCM with simplified physical parametrizations. I: Model climatology and variability in multi-decadal experiments. Clim. Dyn., 20, 175-191.

Pope, V.D., Gallani, M., Rowntree, P.R., and Stratton, R.A., 2000: The impact of new physical parametrizations in the Hadley Centre climate model - HadAM3. Clim. Dyn., 16, 123-146.

Rayner, N. A., D. E. Parker, E. B. Horton, C. K. Folland, L. V. Alexander, D. P. Rowell, E. C. Kent, and A. Kaplan, 2003: Global analyses of sea surface temperature, sea ice and night marine air temperature since the late nineteenth century. *J. Geophys. Res*., *108(D14*), 4407, doi:10.1029/2002JD002670.

Roeckner E., 1996. The atmospheric general circulation model ECHAM-4: model description and simulation of present-day climate. Max-Planck-Institut fur Meteorologie, Rep. No 218, Hamburg, Germany, 90 pp.

Salas-Melia, D., F. Chauvin, M. Deque, H. Douville, J.F. Gueremy, P. Marquet, S. Planton, J.F. Royer and S. Tyteca (2005) : Description and validation of the CNRM-CM3 global coupled model, CNRM working note 103.

Shin, H.-J., I.-U. Chung, H.-J. Kim, and J.-W. Kim (2006), Global energy cycle between land and ocean in the simulated 20th century climate systems, *Geophys. Res. Lett.*, 33, L14702, doi:10.1029/2006GL025977.

Sutton, R. T., B.-W. Dong, and J. M. Gregory, 2007: Land/sea warming ratio in response to climate change: IPCC AR4 model results and comparison with observations. Geophys. Res. Lett., 34, L02701, doi:10.1029/2006GL028164.

Thompson, D.W.J., J.M. Wallace and G.C. Hegerl, 2000: Annual modes in the extratropical circulation Part II: trends. *J. Climate*, 13, 1018-1036.

Winton, M., 2006: Amplified Arctic climate change: What does surface albedo feedback have to do with it? *Geophys. Res. Lett.*, 33, L03701, doi:10.1029/2005GL025244.